Outer-Sphere Effects on Reduction Potentials of Copper Sites in Proteins: The Curious Case of High Potential Type 2 C112D/M121E *Pseudomonas aeruginosa* Azurin

Kyle M. Lancaster[1,*], **Stephen Sproules**[2], **Joshua H. Palmer**[1], **John H. Richards**[1,*], and **Harry B. Gray**[1,*]

[1]Beckman Institute, California Institute of Technology, Pasadena, CA, USA 91125

[2]Max-Planck-Institut für Bioanorganische Chemie, Stiftstrasse 34-36, D-45470 Mülheim an der Ruhr, Germany

Abstract

Redox and spectroscopic (electronic absorption, multifrequency electron paramagnetic resonance (EPR), and X-ray absorption) properties together with X-ray crystal structures are reported for the type 2 Cu^{II} C112D/M121E variant of *Pseudomonas aeruginosa* azurin. The results suggest that Cu^{II} is constrained from interaction with the proximal glutamate; this structural frustration implies a "rack" mechanism for the 290 mV (vs NHE) reduction potential measured at neutral pH. At high pH (~ 9), hydrogen bonding in the outer coordination sphere is perturbed to allow axial glutamate ligation to Cu^{II}, with a decrease in potential to 119 mV. These results highlight the role played by outer-sphere interactions, and the structural constraints they impose, in determining the redox behavior of transition metal protein cofactors.

Introduction

Blue (type 1) copper proteins are key players in a great many biological electron transfer (ET) reactions.[1–2] Type 1 sites, which contain a trigonal N-N-S ligand set (two histidines and a cysteine), with axial ligation from either a methionine or glutamine at the "south pole" and in some cases a backbone carbonyl at the "north pole," exhibit intense (ε ~ 5000 $M^{-1}cm^{-1}$) thiolate π to Cu d_{x2-y2} ligand to metal charge transfer (LMCT) absorption near 600 nm and narrow axial EPR hyperfine splitting ($A_{\parallel}$ 9.5 mK). These optical and EPR spectroscopic properties have been ascribed to a highly covalent S-Cu interaction, which is thought to lower the ET reorganization energy (λ ~ 0.7 eV) as well as enhance distant electronic coupling to the site.[3–5] Further and arguably more significant contributions to the low λ are outer-sphere noncovalent interactions that include hydrogen bonds to the cysteine sulfur. These outer-sphere interactions constrain the coordination geometry of blue copper sites and allow their rapid electron transfer reactivities.[2,6–9]

The $Cu^{II/I}$ reduction potentials of type 1 sites span a wide range, from +200 mV to +1.0 V (or even greater) vs. the normal hydrogen electrode (NHE). This tunability permits T1 sites to participate in ET at favorable driving forces with many different redox partners. Many factors[10] have been invoked as contributors to this modulation of redox potentials,

including: axial ligation;[11−14] site hydrophobicity;[14−16] outer-sphere coordination (hydrogen bonding);[17] and electrostatics.[18] Lu and coworkers recently demonstrated the additive nature of these effects in their work on a series of *Pseudomonas aeruginosa* azurin mutants whose reduction potentials span a range of 600 mV.[19]

We have investigated the applicability of these principles to a type 2 copper site formed by the C112D (C = cysteine, D = aspartate) mutant in *Pseudomonas aeruginosa* azurin.[20−21] Our initial efforts focused on M121 (M = methionine) substitutions, M121X (X = L, H, E) (L = leucine, H = histidine, E = glutamate), where at pH 7.0 we found elevated reduction potentials, 170 mV (single mutant) to ~ 300 mV. The latter value is surprisingly close to that of the wild-type protein. The C112D/M121L mutant gives rise to the type zero copper electronic structure; the elevated reduction potential has thus been ascribed as a consequence of this perturbation combined with increased site hydrophobicity.[22] In the case of C112D/M121H it is likely that a protonated imidazolium side chain of histidine elevates the reduction potential through repulsive electrostatic interaction with the oxidized type 2 center. Following this line of reasoning, coordination to a negatively charged carboxylate would result in a reduction potential for the C112D/M121E variant that should be much lower than the measured value of 290 mV. We have now more extensively characterized C112D/M121E azurin to understand the origin of its surprisingly high reduction potential.

Materials and Methods

Protein Expression and Purification

C112D/M121E azurin was expressed and purified as described previously.[21] *Pseudomonas aeruginosa* cytochrome c_{551} (c_{551}) was expressed recombinantly in dual-transformed *E. coli* BL21(DE3): one plasmid contained the periplasmically-tagged c_{551} gene while a second plasmid bore eight genes to facilitate protein biosynthesis.[23] A 50 mL starter culture in LB medium was incubated with shaking for 24 h at 37 °C. This culture was harvested, resuspended in TB medium, and added to 6 L TB medium (3x 2 L cultures in 6 L Erlenmeyer flasks). The expression culture was incubated at 37°C with shaking for 15 h. Protein was extracted following culture harvesting by osmotic shock. Extract was concentrated in an Amicon fitted with a YM-10 membrane and exchanged into 10 mM Tris pH 7.6 by repeated dilution/concentration. The solution was then loaded onto a batch column packed with DEAE Sepharose FF; protein was eluted with a stepwise gradient from 10–40 mM Tris. The solution was acidified with glacial acetic acid to pH 4.0 and precipitate isolated by centrifugation. Buffer was then exchanged to 25 mM sodium acetate pH 4.0 by desalting column. The solution was loaded onto a SP Sepharose FPLC column and eluted by pH gradient from 4–7. The protein was determined to be homogeneous by silver-stained PAGE; identity was verified by UV/vis and ESI-MS.

Redox Titrations

In a typical experiment, an aliquot of c_{551} was reduced by addition of sodium dithionite to 1 mM. This protein was then desalted into the appropriate buffer. To a 1 cm quartz cuvette was added buffer of appropriate pH and c_{551} to ~8 μM. Final solution volume was 2 mL. This solution was titrated with a ~ 500 μM solution of Cu^{II} C112D/M121E azurin in MilliQ water. Data were fit to the following expression:

$$(Fe^{III}) = \frac{1}{2 \times (K_{eq} - 1)}$$
$$\times K_{eq} \left(\frac{V_{add}}{V_{add}+V_i} \times \left[Cu^{II} \right] + \frac{V_i}{V_{add}+V_i} \times \left[Fe^{II} \right] \right)$$
$$- \left(K_{eq}^2 \times \frac{V_{add}}{V_{add}+V_i} \times \left[Cu^{II} \right] + \frac{V_i}{V_{add}+V_i} \times \left[Fe^{II} \right] \right)^2$$
$$- 4 \times \left(K_{eq} - 1 \right) \times \left(K_{eq} \times \left(\frac{V_{add}}{V_{add}+V_i} \times \left[Cu^{II} \right] + \frac{V_i}{V_{add}+V_i} \times \left[Fe^{II} \right] \right)^{1/2} \right) \tag{1}$$

where V_{add} is the volume of Cu^{II} C112D/M121E azurin added, V_i is the initial volume (2 mL), $[Fe^{II}]_i$ is the starting c_{551} concentration, and $[Cu^{II}]_i$ is the concentration of the C112D/M121E azurin ($\varepsilon_{310} = 1250$ $M^{-1}cm^{-1}$). Fe^{III} concentrations were calculated as the difference from the percentage of initial Fe^{II} concentration from the ratio of A_{520} to A_{551} according to the following expression:

$$\frac{A_{520}}{A_{551}} = 1.1427 + 0.55401(\%Fe^{II}) - 0.065012(\%Fe^{II})^2 \tag{2}$$

pH dependent reduction potentials for c_{551} were taken from the literature.24

EPR Spectroscopy

Samples were prepared by 1:1 dilution of C112D/M121E holoazurin in water with 100 mM CHES (pH 9.0, pH 10.0), HEPES (pH 8.0, pH 7.0), or MES (pH 5.5). Glycerol was then added to 50% to facilitate glassing. Continuous wave (CW) X-band EPR spectra were recorded at 77 K on a Bruker EMX Biospin fitted with a liquid nitrogen cold finger. CW Q-band spectra were measured using a Bruker ESP-300E spectrometer with a Bruker Q-band cavity (ER5106QT) with Bruker flexline support and an Oxford Instruments helium cryostat (CF935). Microwave frequencies were measured with a Hewlett-Packard frequency counter (HP5352P), and the field control was calibrated with a Bruker NMR field probe (ER035M). Sample concentrations were ~1 mM. Spectra were simulated in SPINCOUNT.25

X-ray Absorption Spectroscopy

Cu K-edge X-ray absorption spectra (XAS), including a truncated extended x-ray absorption fine structure (EXAFS) region for normalization, were collected at the Stanford Synchrotron Radiation Lightsource at beam line 7-3 under ring conditions of 3 GeV and 200 mA. A Si(220) double-crystal monochromator was used for energy selection and a Rh-coated mirror (set to an energy cutoff of 13 keV) was used for harmonic rejection. Internal energy calibration was performed by assigning the first inflection point of a Cu foil spectrum to 8980.3 eV. Samples for XAS were prepared as for EPR spectroscopy, though only at pH 5.5, 7.0, and 10.0. Following addition of glycerol, samples were concentrated to ~3 mM. Proteins were loaded into 2 mm Delrin XAS cells with 38 μM Kapton windows and glassed by rapid immersion in liquid nitrogen. Data were collected in fluorescence mode (using a Canberra Ge 30-element array detector) windowed on the Cu Kα emission line. The sample was maintained at 10 K in an Oxford liquid helium flow cryostat. To minimize photoreduction of Cu(II), the incident beam intensity was attenuated by a factor of 3 with a four-layer aluminum Reynolds filter. Data were collected from 8660 to 9380 eV (k = 10 Å^{-1}) to reduce collection time and thus photoreduction. Only one scan per 1 mm × 10 mm spot was averaged per sample. Scans were averaged and processed using the MAVE and PROCESS modules of the EXAFSPAK software package.26

X-ray Crystallography

Crystal growth procedures for C112D/M121X azurins have been reported previously.[22,27] All X-ray diffraction experiments were carried out at the Caltech Molecular Observatory. Procedures for data collection, processing, and structural refinement followed a reported protocol.[22] Coordinates and structure factors have been deposited in the RCSB Protein Data Bank, PDBIDs: 3NP3 (pH 7.0), 3NP4 (pH 9.0).

Results and Discussion

Reduction potentials for C112D/M121E azurin were calculated from equilibrium concentrations obtained from titrations with reduced c_{551} from pH 5.5 to 10.0 (Figure 1). Representative titration data are included in Supporting Information. Cytochrome c_{551} is an exceptional reagent for such titrations as it is intensely colored, displays easily quantifiable oxidation state changes, and is naturally suited for reactivity with azurin as its native ET partner. The pH range was chosen to make use of the noncoordinating buffers (MES, HEPES, and CHES) that avoid complications from buffer-driven metal coordination equilibria. Similar ionic strengths were used to minimize medium effects on equilibrium positions.

The unexpectedly high reduction potential of C112D/M121E azurin is maintained across the range pH 6.0 to 7.5. Below pH 6.0 the reduction potential begins to increase (319 ± 5 mV at pH 5.5). From pH 7.5 to 10.0 there is a precipitous drop in reduction potential from 292 ± 9 to 117 ± 1 mV with an apparent $pK_a \sim 9$. Since the pK_a of the glutamate carboxylate is 4.25,[28] it is unlikely that this dramatic drop arises from a simple on-off ligation effect due to E121 protonation state. Rather, we attribute the rise in potential beginning ~ pH 5.5 to protonation of nonligated E121. In the native protein, a 50 mV decrease in reduction potential is observed as the pH is raised from 5.5 to 8.0.[29] This arises due to deprotonation and thus removal of a positive charge from H35's imidazole sidechain.[30] Lu and co-workers have demonstrated the additive nature of factors that tune the azurin reduction potential;[19] as such in C112D/M121E azurin the 175 mV drop in potential then likely represents both H35 deprotonation and ligation of the E121 carboxylate to Cu^{II}. This explanation for the increased drop in reduction potential does not come as a surprise given previous work on M121E azurin, which demonstrated vast electronic structural perturbations upon deprotonation of the axial carboxylic acid; the implication being that this event is the sole barrier to axial ligation.[31−35] However, our finding that the reduction potential remains as high as 290 mV in the presence of what should be a Cu^{II}-stabilizing axial carboxylate is puzzling, a subject to which we now turn.

Spectroscopic and Structural Properties

The X-band (9.75 GHz) EPR spectrum of a glassed pH 7.0 solution of C112D/M121E azurin recorded at 77 K displays a cluttered $g_\parallel$ region (Figure 2a). A spectrum of the same sample recorded at Q-band (34 GHz) separates this absorption into two field-dependent four-line patterns, indicating that the pH 7.0 X-band spectrum arises from a mixture of two Cu^{II} species (Figure 2b). This obviates the possibility of attributing the fine structure of the $g_\parallel$ region to superhyperfine splitting from the carboxylate proton, thus supporting ligation-state rather than protonation-state equilibrium modulation of the $Cu^{II/I}$ reduction potential.

X-band EPR spectra were recorded in noncoordinating buffers (MES, HEPES, CHES) across the pH range 5.5 to 10 (Figure S3). Spectra corresponding to single species observed at the extrema of this range were simulated using the SPINCOUNT[25] package (Table 1, Figure 3). Fine structure observed in $g_\perp$ arises from a mixture of Cu $A_\perp$ and $A_{N\perp}$;[36] within the limits of the X-band experiment their contributions cannot be deconvoluted and as such

these spectroscopic features were not simulated. The pH 5.5 species has a typical axial type 2 Cu^{II} EPR signature. The pH 10.0 species also possesses a type 2 Cu^{II} spectrum, though it displays anisotropy in $g_\perp$. The axial component of the g-tensor (g_z) decreases from 2.311 ± 0.018 to 2.207 ± 0.047, and there is a substantial (4 mK) increase in axial hyperfine splitting (A_z) at higher pH. The wider hyperfine splitting in the pH 10.0 species is likely attributed to an enlarged orbital dipolar contribution to the hyperfine based on its smaller g_z.

Anisotropy in $g_\perp$ in a D_{4h}-type coordination environment can arise from either lifting of $3d_{xz/yz}$ degeneracy (as would be expected upon geometric distortion) or from mixing of $3d_{z2}$ character into the ground state wavefunction.[37] At pH 5.5, $g_\perp$ is isotropic within the precision of the X-band measurement. However, after accounting for error there is a substantial anisotropy is observed upon raising pH to 10.0, with $\Delta g_{x,y} = 0.051$. Without directly observing the energies of the $3d_{x2-y2}$ to $3d_{xz}$ and $3d_{x2-y2}$ to $3d_{yz}$ LF transitions, the origin of this anisotropy is somewhat ambiguous. However, indirect evidence from X-ray diffraction studies suggests $3d_{z2}$ mixing is the operative mechanism (*vide infra*).

The electronic spectrum of C112D/M121E azurin at pH 5.5 displays a weak ($\varepsilon \sim 70$ $M^{-1}cm^{-1}$) Cu^{II} ligand field (LF) absorption band at 12.3 kK; this feature blue shifts to 18.9 kK at pH 10. The dramatically stronger LF at pH 10 most likely is attributable to E121 carboxylate coordination to Cu^{II}.

The Cu K-edge X-ray absorption near edge spectrum (XANES) of C112D/M121E azurin displays a pH dependence (Figure 5). The lowest energy feature is the ~8979 eV Cu 1s to 3d transition.[38] This transition is forbidden in D_{4h}/O_h symmetry (except for some quadrupolar intensity)[39], but can gain intensity either through mixing of Cu 4p character into the ground state upon distortion to T_d symmetry. We used this effect to quantify the degree of tetrahedral distortion present in the various type zero azurins by correlating the peak intensity with the Cu-O(G45) crystallographically determined bond distance.[22] The 1s to 3d XANES band of C112D/M121E azurin gains no intensity across the observed pH range; rather, it remains very weak. This indicates minimal perturbation to site symmetry, suggesting that 3d orbital energy orderings and by extension degeneracies are preserved. However, the transition maximum shifts ~ 0.7 eV or ~6 kK to higher energy as a consequence of elevating the pH, reflecting increased energy of the frontier Cu^{II} 3d orbital. This shift accords with that observed in the visible spectrum (6.6 kK). As the XANES band corresponds to a transition from the Cu^{II} 1s to the frontier, half-filled 3d orbital, the data suggest that the LF band in the visible spectrum corresponds to a transition from the lowest-energy 3d level to the highest, and that the observed energy change in the visible spectrum reflects a perturbation primarily of the frontier 3d level. The observed shifts in g_z in the EPR spectra are consistent with these 3d energy perturbations.

The second feature displaying a pH dependence is a ~8987 eV shoulder that has been assigned as a "shakedown" transition.[38,40] This transition arises due to orbital contraction resulting from core vacancies following electron promotion. The energy of this transition has been correlated with covalency; lower energy reflects a more covalent site (*i.e.*, one with less Cu^{II} and more ligand character in the ground state). The transition loses intensity and shifts to lower energy upon a rise in pH from 5.5 to 10.0.

Finally, the edge maximum (8995–9000 eV) also shows a pH dependence, which suggests that there is a structural rearrangement of the copper binding site in more basic solutions. An increase in coordination number upon axial carboxylate ligation logically explains this finding.

The redox and spectroscopic data suggest that C112D/M121E azurin adopts two conformations between pH 5.5 and 10.0 with a pK_a of approximately pH 9.0. A pH 7.0

C112D/M121E crystal structure (2.1 Å resolution) revealed one of these conformations (Figure 6a, Table 2). A structure was obtained at pH 9.0 (2.25 Å resolution with acceptable refinement statistics; Figure 6b, Table 2), though there was increased disorder as reflected by elevation of the average thermal factors from 34.733 $Å^2$ (pH 7.0) to 43.827 $Å^2$ (pH 9.0).

Increasing the pH from 7.0 to 9.0 triggers a rearrangement of the Cu^{II} binding site (Table 3). The closest O_e (E121)-Cu^{II} distance decreases from 2.67 to 2.24 Å, indicating a bonding interaction at the higher pH. In the WT protein, the amino nitrogen of H35 is deprotonated at pH 9.0, which leads to a peptide bond flip at P36 as H35 changes from a hydrogen-bond donor (to a backbone carbonyl) to a hydrogen-bond acceptor (from a backbone amide proton).[30] This flip transition occurs with a pK_a of 6.2 in WT azurin, whereas in C112D/M121E azurin, the H35 pK_a is elevated, likely due to close proximity to a neutral metal binding site (as opposed to the monocationic site of WT azurin). Thus, at pH 9.0, the H35-P36 hydrogen bonding network is disrupted, but the peptide bond flip is not observed (Figure 7).[41] However, H35 is dislocated; this adjustment propagates to H46, which allows the Cu^{II} ion to "sink" towards E121, thus establishing ligation (Figure 8). Lengthening of the Cu^{II}-O(G45) distance from 2.62 to 3.24 Å is consistent with this interpretation; the protein is not "loosened" to allow E121 access to the Cu^{II} – rather, the constraint imposed by H46 is relaxed, allowing Cu^{II} access to E121. Concomitant with shortening of the Cu^{II}-O(E121) distance are decreases in Cu^{II}-N(H46/117) distances. These stronger Cu-imidazole interactions likely elevate the $3d_{x2-y2}$ level and thus produce the blue shifted XANES and electronic absorption spectra.

The introduction of E121 as a *bona fide* ligand would lead to overlap between the O 2p/2s orbital's of the carboxylate with the $3d_{z2}$ of Cu^{II}. The ensuing destabilization of $3d_{z2}$ would bring it closer to the frontier $3d_{x2-y2}$ orbital, promoting admixture. Thus the $g_\perp$ anisotropy observed in the pH 10.0 EPR spectrum is likely attributable to $3d_{z2}$ mixing into the frontier molecular orbital wavefunction.

The decrease in reduction potential at elevated pH is, not surprisingly, a consequence of enhanced ligand field strength originating in E121 coordination as well as stronger Cu^{II}-imidazole interactions. That said, the high (~ 300 mV) reduction potential measured between pH 5.5 and 7.5 – even in the presence of a deprotonated axial carboxylate – demands discussion. Previous work on the type 1/1.5 M121H protein[42] implicated protein flexibility as permitting ligation of the engineered axial histidine; in this case ligation was observed to be imidazole protonation state dependent. In short, when it is possible for H121 to ligate Cu^{II}, it will do so. In the present case, the deprotonated E121 is capable of ligating Cu^{II}, but does not. The H35/H46 interaction appears to impose a structural constraint on the protein; thus a rack mechanism is in operation.[2,43] This structural frustration must, as has been proposed time and again for *bona fide* blue copper sites, account for the elevated potential. Though not operating in M121H azurin, rack mechanisms cannot be entirely dismissed in reduction potential tuning of protein-bound copper.

Conclusions

The elevated reduction potential of C112D/M121E azurin at pH 7.0 is attributable to rack-induced structural frustration. Spectroscopic studies demonstrate that axial carboxylate ligation is not protonation-state dependent. pH-dependent X-ray diffraction data reveal that structural constraints on the inner coordination sphere prevent the rearrangement required to permit ligation of Cu^{II} by Glu121. In light of these findings, the rack hypothesis for reduction potential tuning of $Cu^{II/I}$ in azurin should be revisited; comparison to the behavior of M121H azurin suggests that such effects are case dependent, with seemingly subtle structural perturbations leading to vastly different redox behavior. The holistic role of the

protein matrix in tuning the properties of bound metal ion cofactors must be appreciated in order to achieve design mastery over engineered constructs.

Supplementary Material

Refer to Web version on PubMed Central for supplementary material.

Acknowledgments

References

1. Banci, L.; Bertini, I.; Luchinat, C.; Turano, P. Biological Inorganic Chemistry: Structure and Reactivity. Bertini, I.; Gray, HB.; Stiefel, EI.; Valentine, JS., editors. Sausalito: University; 2007. p. 229-277.

2. Gray HB, Malmstrom BG, Williams RJP. J. Biol. Inorg. Chem. 2000; 5:551–559. [PubMed: 11085645]

3. Solomon EI, Szilagyi RK, DeBeer George S, Basumallick L. Chem. Rev. 2004; 104:419–458. [PubMed: 14871131]

4. Gewirth AA, Solomon EI. J. Am. Chem. Soc. 1988; 110:3811–3819.

5. Regan JJ, Di Bilio AJ, Langen R, Skov LK, Winkler JR, Gray HB, Onuchic JN. Chem. Biol. 1995; 2:489–496. [PubMed: 9383451]

6. DeBeer S, Wittung-Stafshede P, Leckner J, Karlsson G, Winkler JR, Gray HB, Malmström BG, Solomon EI, Hedman B, Hodgson KO. Inorg. Chim. Acta. 2000; 297:278–282.

7. Karlsson BG, Aasa R, Malmström BG, Lundberg LG. FEBS Lett. 1989; 253:99–102.

8. Shephard WEB, Anderson BF, Lewandoski DA, Norris GE, Baker EN. J. Am. Chem. Soc. 1990; 112:7817–7819.

9. Crane BR, Di Bilio AJ, Winkler JR, Gray HB. J. Am. Chem. Soc. 2001; 123:11623–11631. [PubMed: 11716717]

10. Li H, Webb SP, Ivanic J, Jensen JH. J. Am. Chem. Soc. 2004; 126:8010–8019. [PubMed: 15212551]

11. Pascher T, Karlsson BG, Nordling M, Malmström BG, Vänngård T. Eur. J. Biochem. 1993; 212:289–296. [PubMed: 8383044]

12. Hall JF, Kanbi LD, Strange RW, Hasnain SS. Biochemistry. 1999; 38:12675–12680. [PubMed: 10504237]

13. Berry SM, Ralle M, Low DW, Blackburn NJ, Lu Y. J. Am. Chem. Soc. 2003; 125:8760–8768. [PubMed: 12862470]

14. Garner DK, Vaughan MD, Hwang HJ, Savelieff MG, Berry SM, Honek JF, Lu Y. J. Am. Chem. Soc. 2006; 128:15608–15617. [PubMed: 17147368]

15. Donaire A, Jiménez B, Moratal J-M, Hall JF, Hasnain SS. Biochemistry. 2001; 40:837–846. [PubMed: 11170402]

16. Donaire A, Jiménez B, Fernández CO, Pierattelli R, Niizeki T, Moratal J-M, Hall JF, Takamitsu K, Hasnain SS, Vila AJ. J. Am. Chem. Soc. 2002; 124:13698–13708. [PubMed: 12431099]

17. Yanagisawa S, Banfield MJ, Dennison C. Biochemistry. 2006; 45:8812–8822. [PubMed: 16846224]

18. Battistuzzi G, Borsari M, Loschi L, Menziani MC, De Rienzo F, Sola M. Biochemistry. 2001; 40:6422–6430. [PubMed: 11371205]

19. Marshall NM, Garner DK, Wilson TD, Gao Y-G, Robinson H, Nilges MJ, Lu Y. Nature. 2009; 462:113–116. [PubMed: 19890331]

20. Mizoguchi TJ, Di Bilio AJ, Gray HB, Richards JH. J. Am. Chem. Soc. 1992; 114:10076–10078.

21. Lancaster KM, Yokoyama K, Richards JH, Winkler JR, Gray HB. Inorg. Chem. 2009; 48:1278–1280. [PubMed: 19113863]

22. Lancaster KM, DeBeer George S, Yokoyama K, Richards JH, Gray HB. Nat. Chem. 2009; 1:711–715. [PubMed: 20305734]

23. Russell BS, Zhong L, Bigotti MG, Cutruzzolà F, Bren KL. J. Biol. Inorg. Chem. 2003; 8:156–166. [PubMed: 12459911]

24. Moore GR, Pettigrew GW, Pitt RC, Williams RJP. Biochim. Biophys. Acta. 1980; 590:261–271. [PubMed: 6245686]

25. Golombek AP, Hendrich MP. J. Magn. Reson. 2003; 165:33–48. [PubMed: 14568515]

26. George, GN. EXAFSPAK. (Stanford Synchrotron Radiation Lightsource, Stanford Linear Accelerator Center, Stanford University);

27. Faham S, Mizoguchi TJ, Adman ET, Gray HB, Richards JH, Rees DC. J. Biol. Inorg. Chem. 2000; 2:464–469.

28. Nelson, DL.; Cox, MM. Lehninger Principles of Biochemistry. 3rd ed.. New York: Worth; 2003.

29. Pettigrew GW, Leitch FA, Moore GR. Biochim. Biophys. Acta. 1983; 725:409–416. [PubMed: 6418204]

30. Nar H, Messerschmidt A, Huber R, van de Kamp M, Canters GW. Crystal Structure Analysis of Oxidized *Pseudomonas aeruginosa* azurin at pH 5.5 and pH 9.0. J. Mol. Biol. 1991; 221:765–772. [PubMed: 1942029]

31. Di Bilio AJ, Chang TK, Malmström BG, Gray HB, Karlsson BG, Nordling M, Pascher T, Lundberg LG. Inorg. Chim. Acta. 1992:145–148.

32. Andrew CR, Yeom H, Valentine JS, Karlsson BG, Bonander N, van Pouderoyen G, Canters GW, Loehr TM, Sanders-Loehr J. J. Am. Chem. Soc. 1994; 116:11489–11498.

33. Strange RW, Murphy LM, Karlsson BG, Reinhammar B, Hasnain SS. Biochemistry. 1996; 50:16391–16398. [PubMed: 8973215]

34. Karlsson BG, Tsai L-C, Nar H, Sanders-Loehr J, Bonander N, Langer V, Sjölin L. Biochemistry. 1997; 36:4089–4095. [PubMed: 9100002]

35. Webb MA, Kiser CN, Richards JH, Di Bilio AJ, Gray HB, Winkler JR, Loppnow GR. J. Phys. Chem. B. 2000; 104:10915–10920.

36. Antholine WE, Hanna PM, McMillin DR. Low Frequency EPR of *Pseudomonas aeruginosa* Azurin. Biophys. J. 1993; 64:267–272. [PubMed: 8381679]

37. Gewirth AA, Cohen SL, Schugar HJ, Solomon EI. Inorg. Chem. 1987; 26:1133–1146.

38. Shadle SE, Penner-Hahn JE, Schugar HJ, Hedman B, Hodgson KO, Solomon EI. J. Am. Chem. Soc. 1993; 115:767–776.

39. Hahn JE, Scott RA, Hodgson KO, Doniach S, Desjardins SR, Solomon EI. Chem. Phys. Lett. 1982; 88:595–598.

40. DeBeer S, Kiser CN, Mines GA, Richards JH, Gray HB, Solomon EI, Hedman B, Hodgson KO. Inorg. Chem. 1999; 38:433–438. [PubMed: 11673945]

41. As the pH 9.0 structure represents a point toward the center of the equilibrium, we collected diffraction data at pH 10.0 to confirm the P36/G37 peptide flip. Despite missing electron density and hence poor refinement statistics, we could unequivocally resolve the structural rearrangement in this region (Figure S4, Tables S1–2).

42. Messerschmidt A, Prade L, Kroes SJ, Sanders-Loehr J, Huber R, Canters GW. Proc. Natl. Acad. Sci. U.S.A. 1998; 95:3443–3448. [PubMed: 9520385]

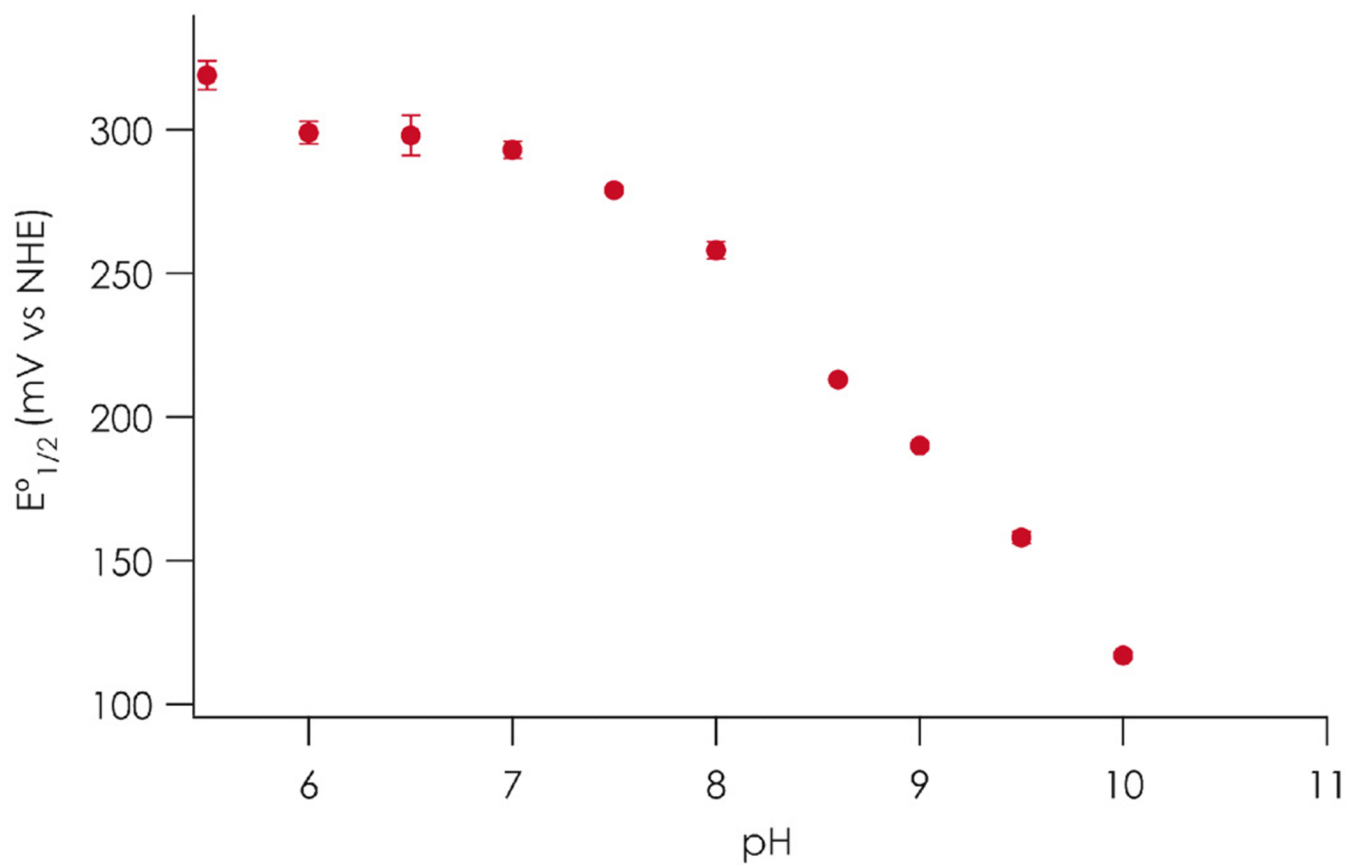43. Malmström BG. Eur. J. Biochem. 1994; 223:711–718. [PubMed: 8055947]

Figure 1.
pH dependence of the C112D/M121E azurin reduction potential (by cytochrome c_{551} titration in aqueous solutions at 298 K). Error bars represent one standard deviation of three titrations.
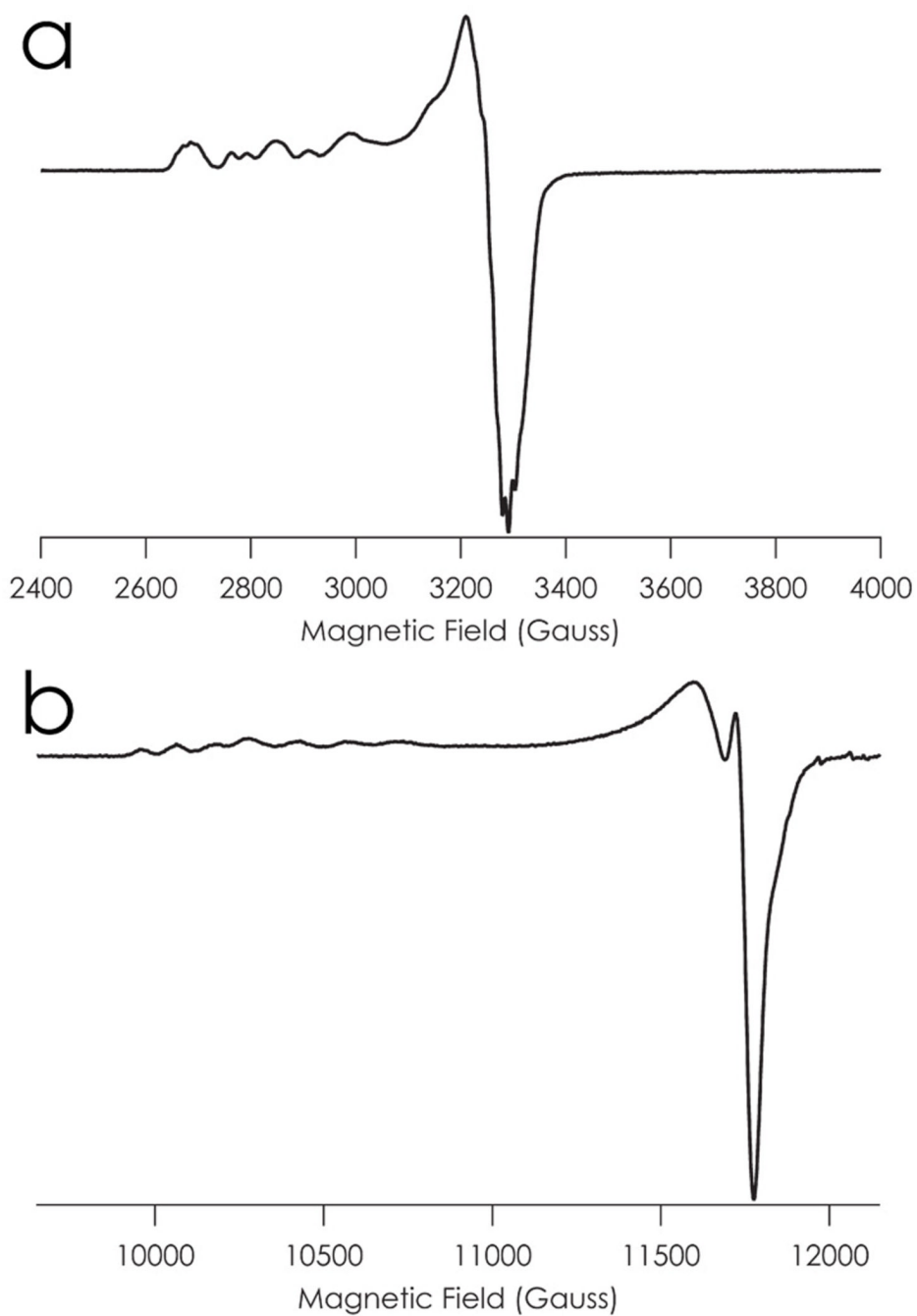
Figure 2.
EPR spectra of C112D/M121E azurin recorded in aqueous 77 K glass at pH 7.0 (50 mM HEPES) at a) X-band and b) Q-band.
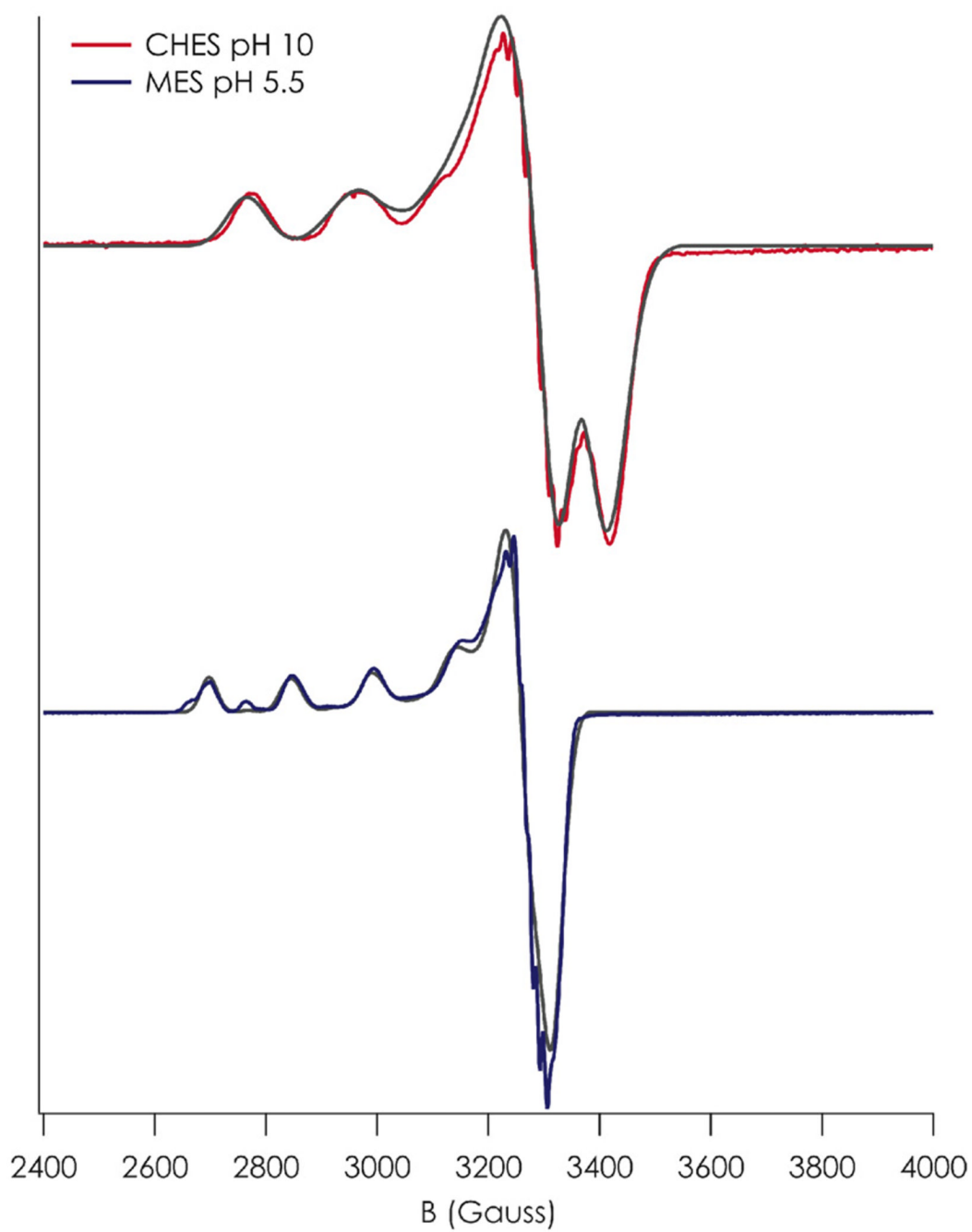
Figure 3.
X-band EPR spectra of C112D/M121E azurin in pH 5.5 (blue) and pH 10.0 (red) aqueous 77 K glass. SPINCOUNT[25] simulations of each spectrum are overlaid in gray.
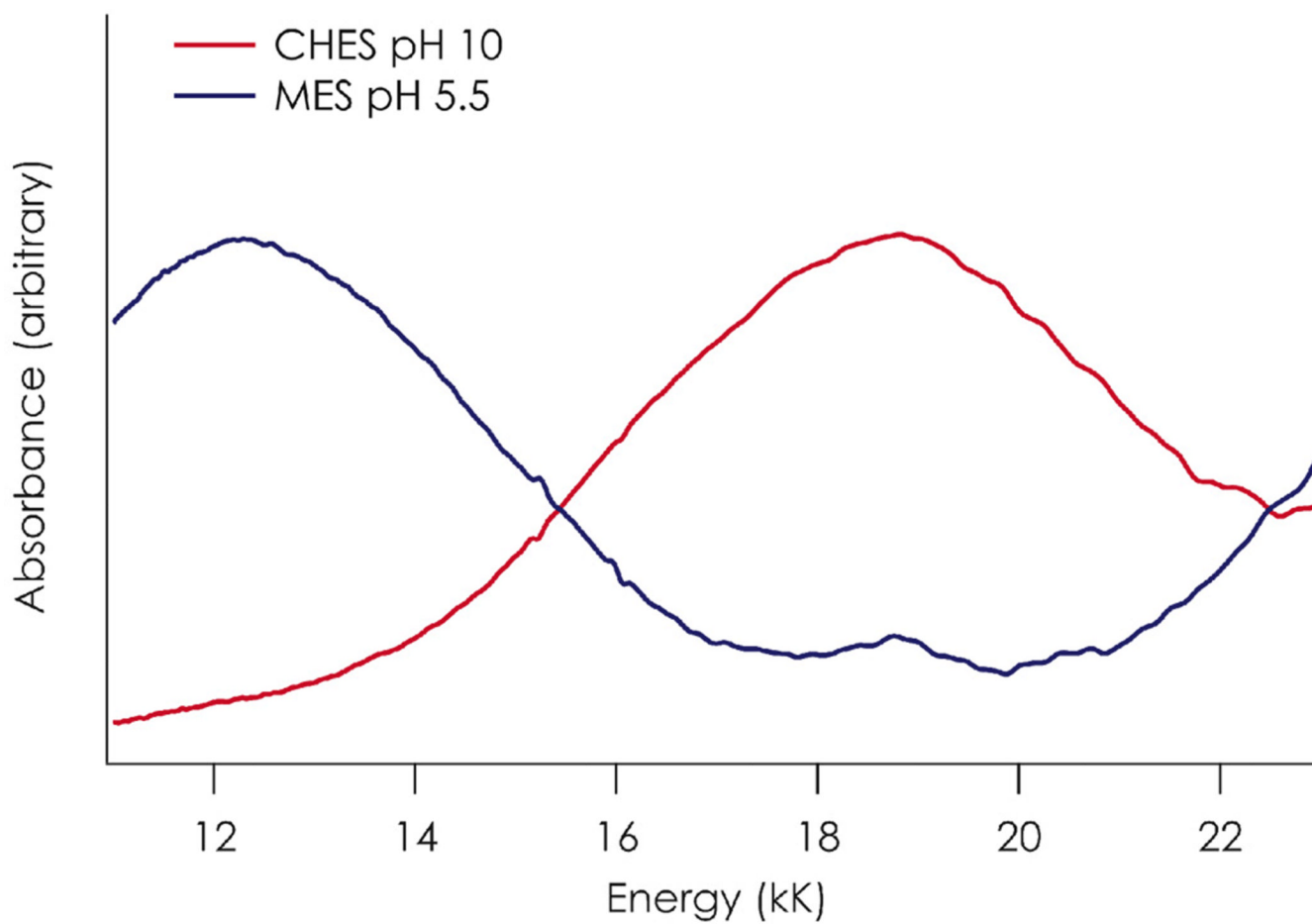
Figure 4.
Electronic absorption spectra of C112D/M121E azurin in pH 5.5 (blue) and 10.0 (red)
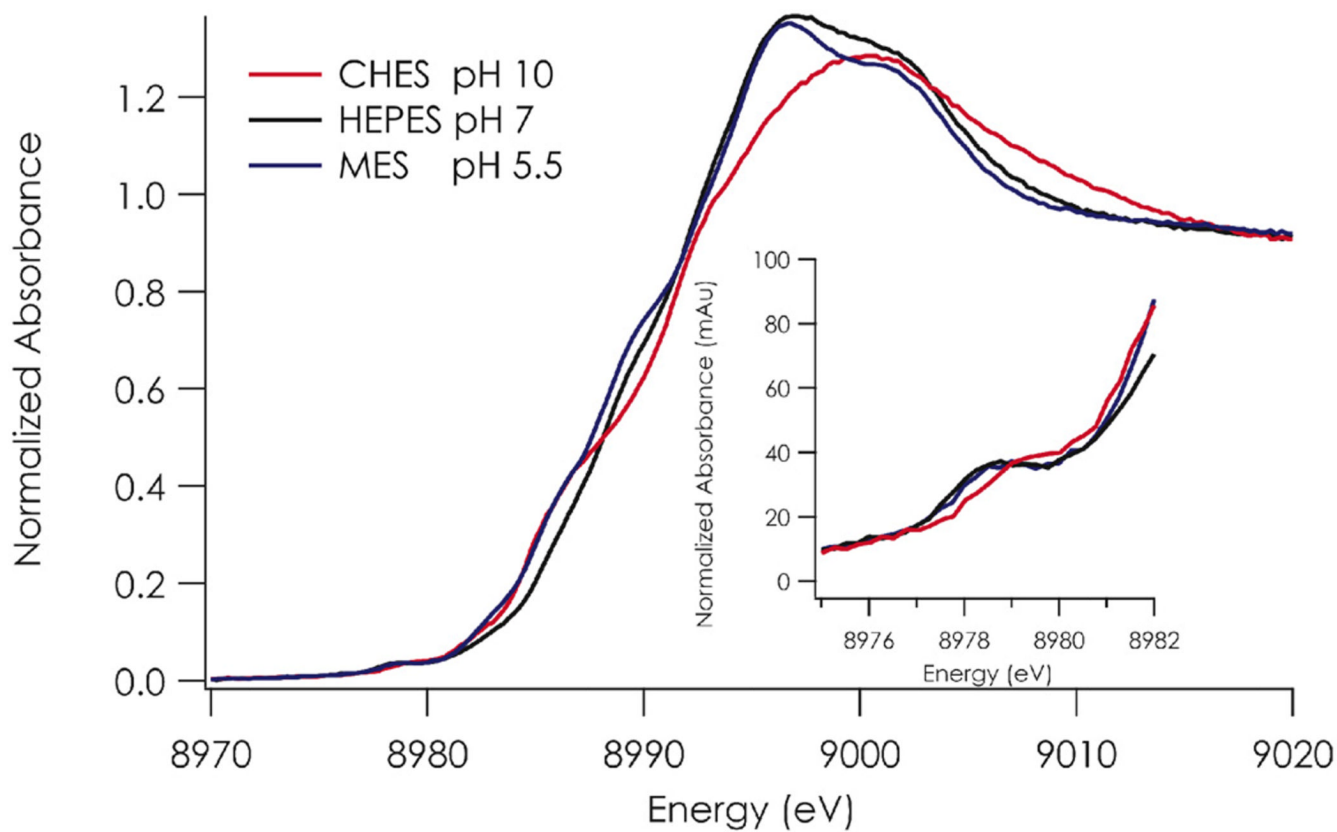aqueous solutions at 298 K.

Figure 5.
Cu K-edge XAS of C112D/M121E azurin at pH 5.5 (blue), 7.0 (black), and 10.0 (red) at 10 K. Inset: the 1s to 3d transition is highlighted.
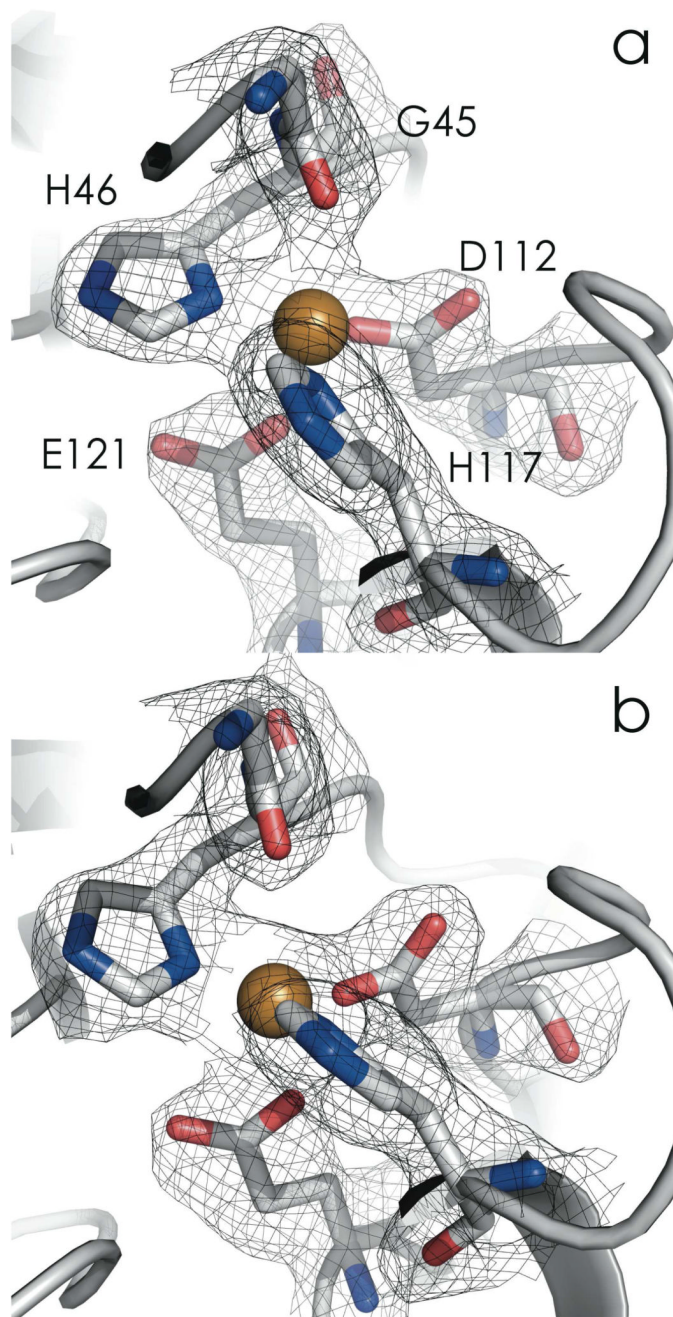
Figure 6.
Cu^{II} active-site region C112D/M121E azurin at pH 7.0 (2.1 Å, a, PDBID: 3NP3) and pH 9.0 (2.25 Å, b, PDBID: 3NP4). $2F_o$-F_c maps are displayed at the 1σ level. Nitrogen atoms are blue; oxygen atoms are red.
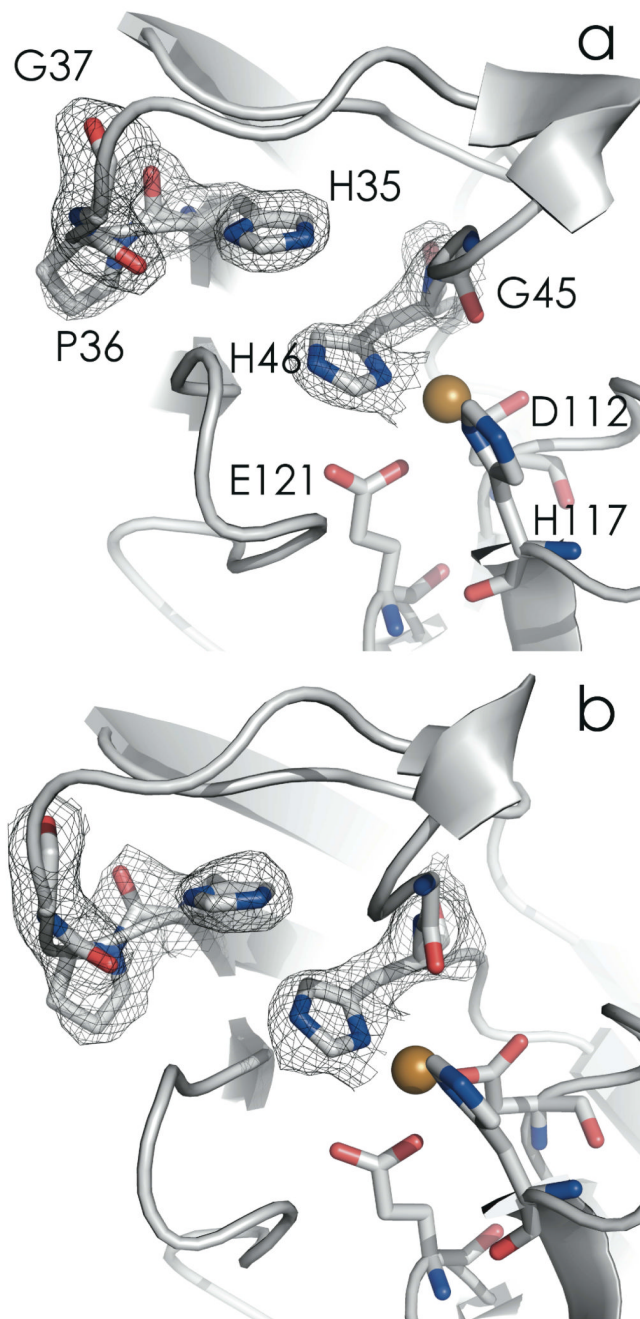
Figure 7.
Active-site region showing the H35-P36 interaction in C112D/M121E azurin at pH 7.0 (2.1 Å, a, PDBID: 3NP3) and pH 9.0 (2.25 Å, b, PDBID: 3NP4). $2F_o$-F_c maps are displayed at the 1σ level. Nitrogen atoms are blue; oxygen atoms are red.
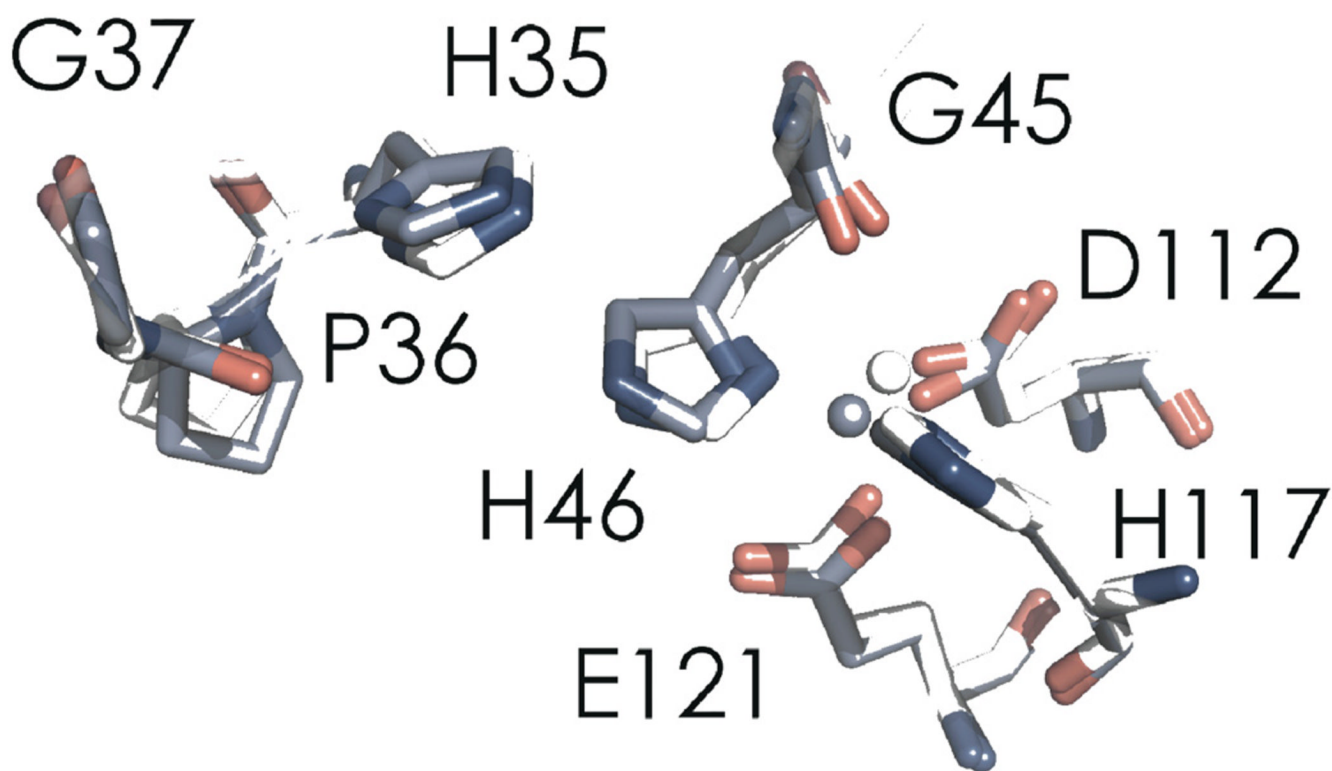
Figure 8.
C_α structural alignment of C112D/M121E azurin at pH 7.0 (2.1 Å, a, PDBID: 3NP3, white) with the structure solved at pH 9.0 (2.25 Å, b, PDBID: 3NP4, slate).

Table 1

Principal Components of Spin Hamiltonian g-Tensor and ^{63,65}Cu (I = 3/2, 100% Abundance) Magnetic Hyperfine Tensor (A, mK[a]) Derived from SPINCOUNT[25] Simulations of X-band EPR spectra at 77K.[b]

pH	g_x	g_y	g_z	σg_x	σg_y	σg_z	A_z(mK)	σA_z(mK)
5.5	2.067	2.067	2.312	0.017	0.017	0.019	15.8	0.1
10	2.027	2.078	2.212	0.017	0.024	0.038	19.8	0.5

[a] 1 mK = 10^{-3} cm^{-1}.

[b] Linewidths were modeled entirely by strain parameters, σg and σA.

Base simulation linewidth was set to 5 G in keeping with a 5 G modulation amplitude used in the experiment.

Table 2

Crystallographic data collection statistics.

	pH 7.0	pH 9.0
Space Group	**C 2 2 2₁**	**C 2 2 2₁**
A	48.86	48.41
B	54.24	55.03
C	94.23	94.58
α	90°	90°
β	90°	90°
γ	90°	90°
Resolution	19.28–2.10 Å	33.93–2.25 Å
Reflections	7238 (534)	5614 (404)
Completeness	99.9% (99.8%)	94.1% (89.8%)
Multiplicity	4.9 (5.0)	3.3 (3.3)
I/sigmaI	6.4 (2.1)	8.7 (5.7)
Rwork	21.4% (23.8%)	21.6% (21.7%)
Rfree	26.5% (27.1%)	27.6% (22.5%)
e.s.u. (work)	0.174 Å	0.218 Å
e.s.u. (free)	0.216 Å	0.278 Å
B$_{average}$	34.733 Å^2	43.827 Å^2

Table 3

Donor-atom distances to Cu^{II} (Å).

	pH 7.0	pH 9.0
O(G45)	2.62	3.24
N(H46)	1.96	1.76
O_{e1}(D112)	1.73	1.72
O_{e2}(D112)	3.25	3.55
N(H117)	2.06	1.99
O_{e1}(E121)	2.67	2.24
O_{e2}(E121)	3.94	3.37